A Servo-Motor-Actuated Artificial Lung for Robotic Speech Production

Ian S. Howard

SECAM, University of Plymouth, Drakes Circus, Plymouth, PL4 8AA, UK.
ian.howard@plymouth.ac.uk

Abstract: Breathing is fundamental to speech production, supplying airflow for both voicing and fricative noise generation. We developed an autonomous robotic lung system that prioritizes functionally relevant, speech-oriented airflow over biological realism, using an accordion-style polyurethane duct actuated by a motor-driven crank–slider mechanism. A kinematic and volumetric analysis is presented that provides a direct, predictive mapping from motor commands to lung displacement and speech-relevant airflow, enabling controlled generation of voiced and unvoiced excitation without requiring a full physiological respiratory model. The system has a tidal volume of approximately 2,000 cm^3, placing it well within the range required for normal adult speech breathing. Experimental results show that the mechanical lung produces inhalation–exhalation cycles and sufficient airflow modulation to support robotic speech production and can drive a simple artificial larynx to generate voicing-like excitation.

1 Introduction

Breathing plays a crucial role in the production of speech. Air expelled from the lungs excites the vocal folds, generating voiced sound within the vocal tract above them. In addition, airflow through narrow constrictions generates fricative noise as a result of turbulent flow.

The design of mechanical lungs falls into three broad categories: speech-oriented physical models, models used in physiology education, and systems that function as ventilators for human patients. Of the existing physical models of speech breathing that mimic the operation of the human lungs, some of the most widely recognized lung–larynx–vocal-tract systems are the educational models developed by Arai [1]. These models are typically manually operated and involve directly pulling down a diaphragm-like structure by hand. The Waseda set of mechanical speech robots employ realistic airflow generated by mechanical lungs and integrate a complete mechanical respiratory system, including lungs, vocal folds, supraglottal tract, and nasal cavity [2]. In addition, hybrid mechanical lung models have been proposed [3]. A more comprehensive mechanical simulator of the respiratory system has also been developed [4].

Rather than reproducing a full physiological model of breathing, we deliberately adopt a minimal airflow model sufficient to predict and control speech-relevant excitation. The design described here more closely aligns with the bellows-based approach adopted in mechanical ventilators. Our aim is to build an autonomous robotic model of speech production designed to prioritize predictable and controllable speech-oriented airflow, rather than biological realism. The primary contribution of this work is a compact, control-oriented model of robotic speech breathing that directly links actuator kinematics to airflow generation through an explicitly derived crank–slider and volumetric framework. Rather than pursuing anatomical fidelity, the system is designed to support precise, repeatable, and speech-relevant airflow modulation suitable for driving artificial laryngeal and vocal-tract models. This approach enables respiratory–laryngeal coordination to be studied and controlled using standard motor commands, while remaining analytically tractable and mechanically simple.

Figure 1. Robotic Lung. Image of the lung apparatus, shown with a simple larynx model attached at the top.

2 Breathing Airflow During Speech

Unlike discrete limb movements, which are often well described by smooth, symmetric minimum-jerk trajectories [5], breathing airflow during speech exhibits characteristic temporal asymmetries, including during text reading [6], and piecewise structure that reflects fundamentally different control objectives [7]. Thus, speech breathing is not organized around producing a smooth kinematic trajectory but around regulating aerodynamic variables—primarily airflow and subglottal pressure—under linguistic, physiological, and biomechanical constraints.

Although this regulation is expressed in terms of aerodynamic variables, the associated lung motion is fully determined by the underlying volumetric dynamics, yielding predictable patterns of lung expansion and compression as a direct consequence of airflow control, rather than as an independently planned kinematic trajectory. Consequently, speech breathing is more naturally characterized as a constrained regulatory control process acting on aerodynamic variables rather than as a kinematic trajectory, a distinction formalized in recent state-space models of airflow and pressure regulation in the human vocal apparatus [8].

3 Mechanical Design

A robotic lung is constructed from commercially available polyurethane 15 cm diameter air-conditioning ducting, which is lightweight, airtight, inexpensive, and easily compressed, making it well-suited for producing reliable volumetric deformation under motor actuation. When fully extended, the duct length was 28 cm and could be compressed to 14 cm by the actuator. The mechanical structure is built from a 20 x 20 mm V-slot aluminum-profile framework, fitted with custom-designed and ABS 3D-printed components (using a Creality K1max printer) that rigidly support the motor, crank–slider assembly, and accordion-style polyurethane lung. Inhalation and exhalation are controlled by compressing and releasing the accordion ducting via a motor-driven crank–slider mechanism. The crank is rotated by an actuator and connected to a slider by a 16mm outer diameter carbon fiber tube rod, which is both very stiff and light.

The slider is attached to the base of the polyurethane accordion structure. The bottom of the accordion is stabilized to follow in a vertical up-and-down motion by 8 mm internal-diameter linear bearings running along cylindrical stainless-steel guide rods, ensuring smooth and purely vertical motion during compression and expansion. Plain bearings were chosen because they operate almost silently, whereas linear ball bearings produce noticeable acoustic noise. The motor is mounted using printed fixtures that ensure accurate alignment with the vertically constrained plunger attached to the base of the accordion structure. A 2 cm diameter hole at the top of the accordion housing allows airflow to exit into an attachable artificial larynx, which is also 3D-printed and slots securely onto the lung outlet. An artificial larynx can be mounted on top of the windpipe to generate pulsatile excitation of the upper structure. In this initial work, a simple larynx model was used as a self-oscillating mechanical model of the vocal folds [9]. It consisted of two pieces of stretched silicone rubber (cut from Suright 2M Resistance Bands). By tuning the tension appropriately and ensuring that the two pieces of rubber are positioned closely together, it is possible to generate a voicing-like excitation.

The rotary actuator (MyActuator DMG X8-H) is controlled via an Adafruit CAN Pal (TJA1051T/3) transceiver driven by a Seeed XIAO ESP32S3 Plus microcontroller, with high-level control running on a laptop PC. By compressing and releasing the accordion structure, air is forced out of this artificial lung into the windpipe above it.

4 Mathematical Modelling of Quasi-Incompressible Gas Dynamics

To interpret the relationship between actuator motion and generated airflow, we adopt a minimal volumetric model under an incompressible flow assumption. This approximation is valid for speech-like airflow regimes, where pressure variations remain small [8], since the increase in air pressure within the cylinder is on the order of only 2% relative to ambient pressure. At higher pressures, this assumption introduces estimation error. Since the present work focuses on controlled, speech-like airflow regimes [10], rather than high-pressure respiratory extremes, the incompressible approximation provides a useful and analytically tractable model. Since the fluid is incompressible to a first approximation, any change in volume must be instantaneously balanced by an equivalent volumetric flow rate.

$$V_{in} = V_0 - xA_p \tag{1}$$

where V_0 is the resting (maximum) volume. Differentiating this equation with respect to time, the rate of change of volume is therefore:

$$\dot{V}_{in} = -\dot{x}A_p \tag{2}$$

So, the airflow rate Q is:

$$\Rightarrow Q = \dot{x}A_p \tag{3}$$

We adopt a simple model of airflow resistance at the cylinder exit, treating it as a pipe leading to the vocal tract. This linear resistance model can be interpreted as a local linearization of the pressure–flow relationship around speech-relevant operating points. The 2 cm outlet diameter defines the dominant geometric contribution to the effective airflow resistance when the larynx is open. At higher airflow rates, nonlinear pressure–flow effects due to turbulence are expected but are outside the operating regime considered here. This resistance arises from friction, turbulence, and other energy-dissipative mechanisms that result in energy losses as the fluid flows through the pipe. Given that the air pressure outside the cylinder is P_{out} in Pa, the air pressure inside the cylinder is P_{in} in Pa, then the airflow rate, Q, out of the cylinder in $m^3.s^{-1}$ is given by the equation:

$$Q = \frac{(P_{in} - P_{out})}{R_{out}} = \dot{x}A_p \tag{4}$$

where R_{out} constitutes the overall air resistance from the larynx, trachea and outlet. Thus, airflow is directly proportional to the rate of volume change induced by actuator motion. Building on this volumetric relationship, a kinematic analysis is presented that explicitly links actuator motion to lung displacement and resulting airflow.

5 Kinematic Analysis of the Slider Displacement

We provide a kinematic analysis of the crank–slider mechanism and explicitly relate actuator angular position and angular velocity to lung displacement and airflow, respectively. By analyzing the velocity and force transmission characteristics of the mechanism, we demonstrate how motor position and velocity commands map directly onto airflow modulation sufficient for generating both voiced and unvoiced excitation.

In a crank–slider mechanism, a crank of length r (7 cm) rotates and is connected to a slider by a connecting rod of length L (27.5 cm). The slider is constrained to move vertically. Here, the x-axis is defined along the vertical direction of slider motion. For the crank–slider mechanism, let: O = (0, 0) be the crank pivot position, A = ($r\cos\theta$, $r\sin\theta$) be the end of the crank, and B = (x, 0) be the vertical position of the slider (which moves along the line y = 0). Since the connecting rod AB has a fixed length L, the distance between points A and B satisfies the expression:

$$(x - r\cos\theta)^2 + (r\sin\theta)^2 = L^2 \tag{5}$$

Leading to the expression:

$$x^2 - 2xr\cos\theta + r^2 - L^2 = 0 \tag{6}$$

Using the quadratic equation formula, this leads to the solution for position x:

$$x = \frac{2r\cos\theta \pm \sqrt{(2r\cos\theta)^2 - 4(r^2 - L^2)}}{2} \tag{7}$$

Taking the meaningful solution for the physical arrangement of the plunger mechanism:

$$x = r\cos\theta + \sqrt{L^2 - r^2\sin^2\theta} \tag{8}$$

We note that re-arranging Equation (6) also leads to the inverse kinematic relationship:

$$\theta = \arccos\left(\frac{x^2 + r^2 - L^2}{2xr}\right) \tag{9}$$

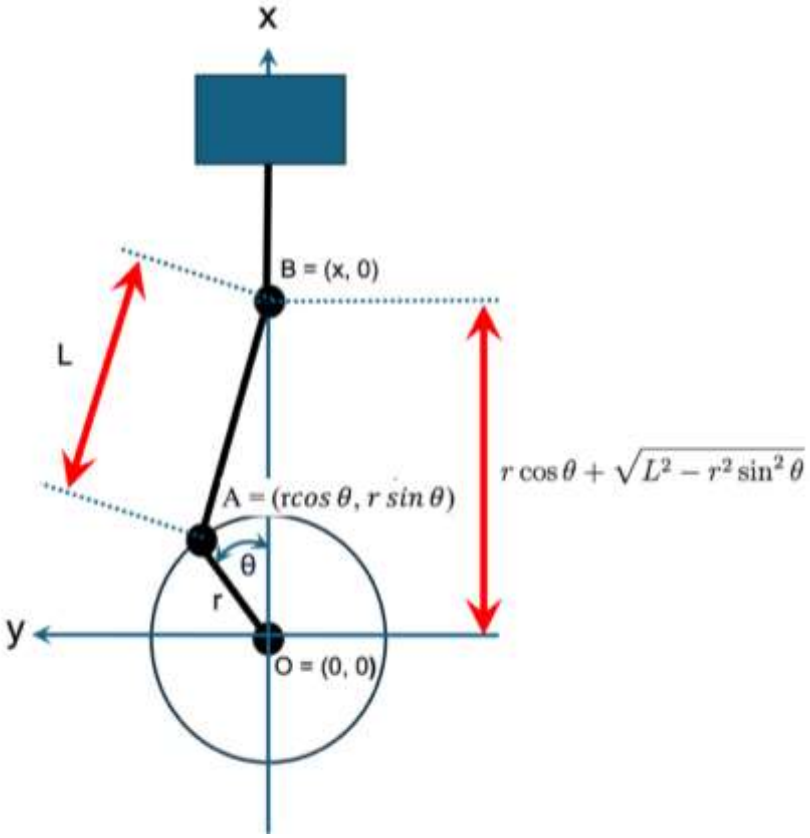

Figure 2 Schematic of a crank mechanism to drive the accordion lung mechanism. For convenience, we define the x-axis to lie along the vertical direction of slider motion. The motor crank radius is 7 cm, and the connecting link rod has a length is 27.5 cm.

6 Crank Mechanism Jacobian

The Jacobian J(θ) is the derivative of the slider displacement with respect to the crank angle θ:

$$J(\theta) = \frac{dx}{d\theta} = \frac{d}{d\theta}\left(r\cos\theta + \sqrt{L^2 - r^2\sin^2\theta}\right) \tag{10}$$

The derivative of the first term is straightforward:

$$\frac{d}{d\theta}(r\cos\theta) = -r\sin\theta \tag{11}$$

To evaluate the derivative of the second term we use the chain rule and define:

$$\frac{dx}{d\theta} = -r\sin\theta + \frac{dx}{du}.\frac{du}{d\theta} \tag{12}$$

Where:

$$u = L^2 - r^2\sin^2\theta \tag{13}$$

$$x = \sqrt{u} \tag{14}$$

So

$$\frac{dx}{du} = \frac{1}{2\sqrt{u}} = \frac{1}{2\sqrt{L^2 - r^2 sin^2\theta}} \tag{15}$$

Again, using the chain rule, we can calculate the term:

$$\frac{du}{d\theta} = -2r^2 sin\,\theta\, cos\,\theta \tag{16}$$

Therefore, we have:

$$\frac{dx}{d\theta} = -r\,sin\,\theta + \frac{1}{2\sqrt{L^2 - r^2 sin^2\theta}} * -2r^2 sin\,\theta\, cos\,\theta \tag{17}$$

$$J(\theta) = -r\,sin\,\theta - \frac{r^2 sin\,\theta\, cos\,\theta}{\sqrt{L^2 - r^2 sin^2\theta}} \tag{18}$$

7 Motor and Plunger Velocity and Force Relationships

To relate motor rotation directly to linear lung motion, we employ the Jacobian of the crank–slider mechanism $J(\theta)$, which depends on the angle θ, to calculate the relationship between the linear velocity of the plunger and the rotational velocity of the motor:

$$\frac{dx}{dt} = J(\theta)\frac{d\theta}{dt} \tag{19}$$

We can also determine the static relationship between the rotary torque T and the linear force F acting on the slider. Assuming a lossless energy conversion, the incremental work done by the torque is equal to the incremental work done on the slider and the Jacobian relationship holds:

$$T = J^T(\theta).F = J(\theta).F \tag{20}$$

Where $J^T(\theta) = J(\theta)$, since the Jacobian for the x-axis motion is a 1x1 matrix. To calculate plunger force, we can use the inverse relationship:

$$F = J^{-1}(\theta).T \tag{21}$$

If we ignore elastic restoring forces of the polyurethane duct, then:

$$F = A_p\,(P_{in} - P_{out}) \tag{22}$$

Therefore:

$$\mathrm{F} = \dot{x}\,R_{out} \tag{23}$$

8 Results

A simple simulation was performed using the derived kinematic and airflow model to illustrate the relationship between actuator motion and generated airflow (Fig. 3). No attempt was made to estimate internal pressure; instead, motor control variables were inferred from actuator kinematics.

Two representative inhalation–exhalation cycles were generated by specifying constant exhalation and inhalation airflow phases with smooth transitions to ramp them up and down (Fig.

3A). These airflow rates represent suitable values for speech production. Air displacement was directly obtained by integrating the air flow rate (Fig. 3B), which also directly determined plunger position. Inverse kinematics were used to calculate the corresponding angle (Fig. 3C) and angular velocity (Fig. 3D) of the motor driving the crank. The purpose of this simulation was not to estimate absolute internal pressure or precisely calibrate airflow magnitude, but to demonstrate a predictable and repeatable mapping between motor commands and speech-relevant airflow profiles. The simulated airflow profiles fall well within the range typically reported for conversational speech (order of 0.1–0.5 $L \cdot s^{-1}$).

The system produces a tidal volume of approximately 2,000 cm^3, comparable to that of an adult male during normal conversational breathing. Compression of the accordion forces air into the artificial trachea, allowing a simple silicone-rubber larynx to generate voicing-like excitation patterns when membrane tension and spacing are appropriately adjusted. The airflow levels generated are sufficient to drive a range of artificial larynx configurations, consistent with other models used in vocal tract modelling. Because the simulation is derived directly from the mechanism geometry, the same mapping applies to the physical system shown in the supplementary videos. These demonstrate inhalation–exhalation cycles and excitation of simple laryngeal elements under actuator control. These videos are intended as qualitative demonstrations of airflow controllability rather than quantitative acoustic evaluation.

https://www.youtube.com/playlist?list=PLjKvJX8cBCKW_vFdupebHMWzM16khmfcs

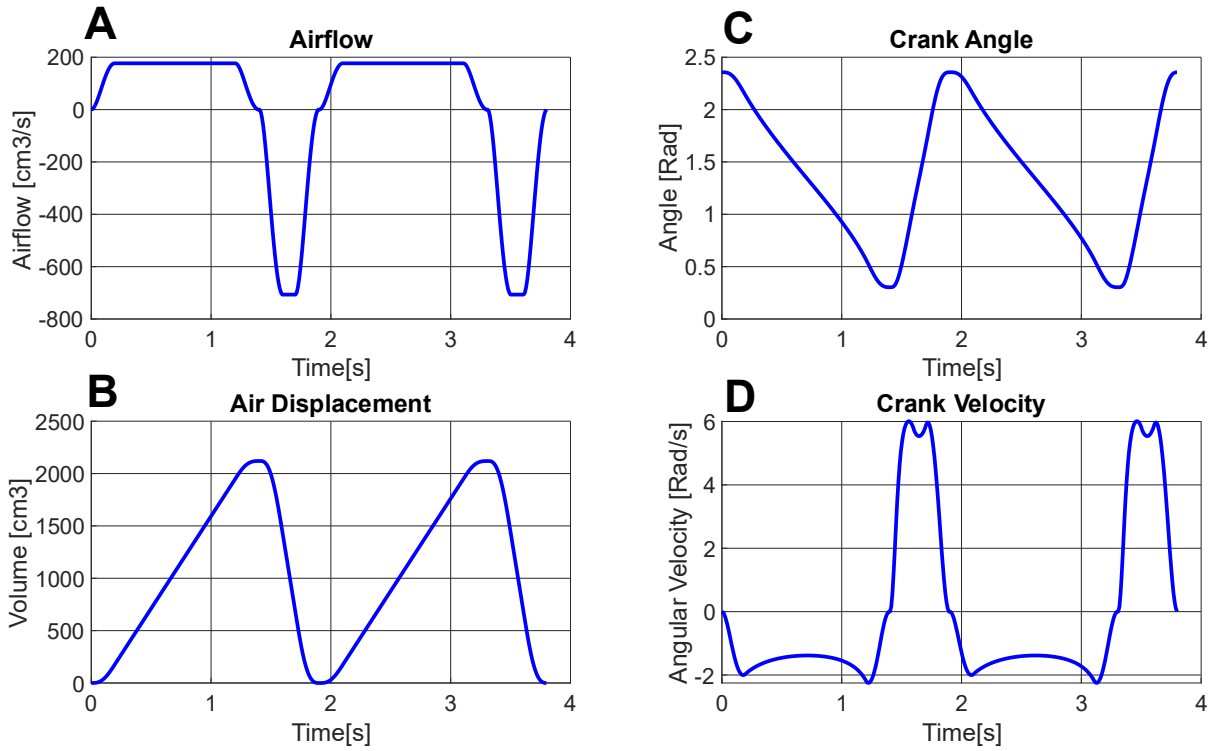

Figure 3. (A) Simulated airflow, (B) air displacement, (C) motor crank angle, and (D) motor angular velocity**.** Motor position and velocity commands were obtained via inverse kinematics to produce plunger trajectories.

9 Conclusions

Experimental recordings of actuator signals and acoustic output demonstrate that controlled crank motion reliably generates inhalation–exhalation cycles with smooth, speech-appropriate airflow modulation. The kinematic framework provides a direct and predictive mapping from

motor commands to airflow, offering a flexible and controllable platform for robotic speech production and respiratory–laryngeal coordination research [11–13]. By expressing speech breathing as a controllable volumetric process driven by actuator kinematics, the system provides a practical link between motor control theory and physical speech synthesis.

Future work will incorporate real-time control of subglottal pressure and acoustic feedback to actively regulate and maintain vocal-fold excitation during speech production. Ultimately, the apparatus will serve as the primary source of controlled airflow for a speaking robotic vocal tract.

10 References

[1] ARAI, TAKAYUKI: Lung model and head-shaped model with visible vocal tract as educational tools in acoustics. In: *Acoustical Science and Technology* Bd. 27 (2006), Nr. 2, S. 111–113

[2] NISHIKAWA, K.; TAKANOBU, H.; MOCHIDA, T.; HONDA, M.; TAKANISHI, A.: Development of a new human-like talking robot having advanced vocal tract mechanisms. In: *Proceedings 2003 IEEE/RSJ International Conference on Intelligent Robots and Systems (IROS 2003) (Cat. No.03CH37453)*. Bd. 2, 2003, S. 1907–1913 Bd.2

[3] PASTEKA, RICHARD; FORJAN, MATHIAS; SAUERMANN, STEFAN; DRAUSCHKE, ANDREAS: Electro-mechanical Lung Simulator Using Polymer and Organic Human Lung Equivalents for Realistic Breathing Simulation. In: *Scientific Reports* Bd. 9, Nature Publishing Group (2019), Nr. 1, S. 19778

[4] GIANNACCINI, MARIA ELENA; HINITT, ANDREW; STINCHCOMBE, ANDREW; YUE, KEREN; BIRCHALL, MARTIN; CONN, ANDREW; ROSSITER, JONATHAN: A Bioinspired Active Robotic Simulator of the Human Respiratory System. In: *IEEE Transactions on Medical Robotics and Bionics* Bd. 5 (2023), Nr. 2, S. 442–454

[5] FLASH, TAMAR; HOGAN, NEVILLE: The coordination of arm movements: an experimentally confirmed mathematical model. In: *Journal of Neuroscience* Bd. 5, Society for Neuroscience (1985), Nr. 7, S. 1688–1703

[6] ROCHET-CAPELLAN, AMÉLIE; FUCHS, SUSANNE: Changes in breathing while listening to read speech: the effect of reader and speech mode. In: *Frontiers in Psychology* Bd. 4, Frontiers (2013)

[7] OHALA, JOHN J.: Respiratory Activity in Speech. In: HARDCASTLE, W. J. ; MARCHAL, A. (Hrsg.): *Speech Production and Speech Modelling*. Dordrecht : Springer Netherlands, 1990 — ISBN 978-94-009-2037-8, S. 23–53

[8] HOWARD, IAN S.: State space model of airflow in the human vocal apparatus. In: *Konferenz Elektronische Sprachsignalverarbeitung* : TUDpress, Dresden, 2025 — ISBN 978-3-95908-803-9, S. 180–187

[9] TITZE, I. R.: The physics of small-amplitude oscillation of the vocal folds. In: *The Journal of the Acoustical Society of America* Bd. 83 (1988), Nr. 4, S. 1536–1552

[10] STEVENS, KENNETH N.; KEYSER, S. J. (Hrsg.): *Acoustic Phonetics*, *Current Studies in Linguistics*. Cambridge, MA, USA: MIT Press, 2000 — ISBN 978-0-262-69250-2

[11] OHALA, JOHN: A mathematical model of speech aerodynamics. In: *Annual Report of the Institute of Phonetics of the University of Copenhagen* Bd. 8 (1974)

[12] HIXON, THOMAS J.; WEISMER, GARY; HOIT, JEANNETTE D.: *Preclinical Speech Science: Anatomy, Physiology, Acoustics, and Perception, Third Edition* : Plural Publishing, 2018. — Google-Books-ID: SDFtDwAAQBAJ — ISBN 978-1-63550-062-2

[13] ZHANG, ZHAOYAN: Respiratory Laryngeal Coordination in Airflow Conservation and Reduction of Respiratory Effort of Phonation. In: *Journal of Voice: Official Journal of the Voice Foundation* Bd. 30 (2016), Nr. 6, S. 760.e7-760.e13